

Proceedings of the 12th International Conference on
Computational Fluid Dynamics in the Oil & Gas,
Metallurgical and Process Industries

Progress in Applied CFD – CFD2017



SINTEF Proceedings

Editors:

Jan Erik Olsen and Stein Tore Johansen

Progress in Applied CFD – CFD2017

Proceedings of the 12th International Conference on Computational Fluid Dynamics
in the Oil & Gas, Metallurgical and Process Industries

SINTEF Academic Press

SINTEF Proceedings no 2

Editors: Jan Erik Olsen and Stein Tore Johansen

Progress in Applied CFD – CFD2017

Selected papers from 10th International Conference on Computational Fluid Dynamics in the Oil & Gas, Metallurgical and Process Industries

Key words:

CFD, Flow, Modelling

Cover, illustration: Arun Kamath

ISSN 2387-4295 (online)

ISBN 978-82-536-1544-8 (pdf)

© Copyright SINTEF Academic Press 2017

The material in this publication is covered by the provisions of the Norwegian Copyright Act. Without any special agreement with SINTEF Academic Press, any copying and making available of the material is only allowed to the extent that this is permitted by law or allowed through an agreement with Kopinor, the Reproduction Rights Organisation for Norway. Any use contrary to legislation or an agreement may lead to a liability for damages and confiscation, and may be punished by fines or imprisonment

SINTEF Academic Press

Address: Forskningsveien 3 B
 PO Box 124 Blindern
 N-0314 OSLO

Tel: +47 73 59 30 00

Fax: +47 22 96 55 08

www.sintef.no/byggforsk

www.sintefbok.no

SINTEF Proceedings

SINTEF Proceedings is a serial publication for peer-reviewed conference proceedings on a variety of scientific topics.

The processes of peer-reviewing of papers published in SINTEF Proceedings are administered by the conference organizers and proceedings editors. Detailed procedures will vary according to custom and practice in each scientific community.

PREFACE

This book contains all manuscripts approved by the reviewers and the organizing committee of the 12th International Conference on Computational Fluid Dynamics in the Oil & Gas, Metallurgical and Process Industries. The conference was hosted by SINTEF in Trondheim in May/June 2017 and is also known as CFD2017 for short. The conference series was initiated by CSIRO and Phil Schwarz in 1997. So far the conference has been alternating between CSIRO in Melbourne and SINTEF in Trondheim. The conferences focuses on the application of CFD in the oil and gas industries, metal production, mineral processing, power generation, chemicals and other process industries. In addition pragmatic modelling concepts and bio-mechanical applications have become an important part of the conference. The papers in this book demonstrate the current progress in applied CFD.

The conference papers undergo a review process involving two experts. Only papers accepted by the reviewers are included in the proceedings. 108 contributions were presented at the conference together with six keynote presentations. A majority of these contributions are presented by their manuscript in this collection (a few were granted to present without an accompanying manuscript).

The organizing committee would like to thank everyone who has helped with review of manuscripts, all those who helped to promote the conference and all authors who have submitted scientific contributions. We are also grateful for the support from the conference sponsors: ANSYS, SFI Metal Production and NanoSim.

Stein Tore Johansen & Jan Erik Olsen



Organizing committee:

Conference chairman: Prof. Stein Tore Johansen

Conference coordinator: Dr. Jan Erik Olsen

Dr. Bernhard Müller

Dr. Sigrid Karstad Dahl

Dr. Shahriar Amini

Dr. Ernst Meese

Dr. Josip Zoric

Dr. Jannike Solsvik

Dr. Peter Witt

Scientific committee:

Stein Tore Johansen, SINTEF/NTNU

Bernhard Müller, NTNU

Phil Schwarz, CSIRO

Akio Tomiyama, Kobe University

Hans Kuipers, Eindhoven University of Technology

Jinghai Li, Chinese Academy of Science

Markus Braun, Ansys

Simon Lo, CD-adapco

Patrick Segers, Universiteit Gent

Jiyuan Tu, RMIT

Jos Derksen, University of Aberdeen

Dmitry Eskin, Schlumberger-Doll Research

Pär Jönsson, KTH

Stefan Pirker, Johannes Kepler University

Josip Zoric, SINTEF

CONTENTS

PRAGMATIC MODELLING	9
On pragmatism in industrial modeling. Part III: Application to operational drilling	11
CFD modeling of dynamic emulsion stability	23
Modelling of interaction between turbines and terrain wakes using pragmatic approach	29
FLUIDIZED BED	37
Simulation of chemical looping combustion process in a double looping fluidized bed reactor with cu-based oxygen carriers.....	39
Extremely fast simulations of heat transfer in fluidized beds.....	47
Mass transfer phenomena in fluidized beds with horizontally immersed membranes	53
A Two-Fluid model study of hydrogen production via water gas shift in fluidized bed membrane reactors	63
Effect of lift force on dense gas-fluidized beds of non-spherical particles	71
Experimental and numerical investigation of a bubbling dense gas-solid fluidized bed	81
Direct numerical simulation of the effective drag in gas-liquid-solid systems	89
A Lagrangian-Eulerian hybrid model for the simulation of direct reduction of iron ore in fluidized beds.....	97
High temperature fluidization - influence of inter-particle forces on fluidization behavior	107
Verification of filtered two fluid models for reactive gas-solid flows	115
BIOMECHANICS.....	123
A computational framework involving CFD and data mining tools for analyzing disease in carotid artery	125
Investigating the numerical parameter space for a stenosed patient-specific internal carotid artery model.....	133
Velocity profiles in a 2D model of the left ventricular outflow tract, pathological case study using PIV and CFD modeling.....	139
Oscillatory flow and mass transport in a coronary artery.....	147
Patient specific numerical simulation of flow in the human upper airways for assessing the effect of nasal surgery.....	153
CFD simulations of turbulent flow in the human upper airways	163
OIL & GAS APPLICATIONS	169
Estimation of flow rates and parameters in two-phase stratified and slug flow by an ensemble Kalman filter	171
Direct numerical simulation of proppant transport in a narrow channel for hydraulic fracturing application	179
Multiphase direct numerical simulations (DNS) of oil-water flows through homogeneous porous rocks	185
CFD erosion modelling of blind tees	191
Shape factors inclusion in a one-dimensional, transient two-fluid model for stratified and slug flow simulations in pipes	201
Gas-liquid two-phase flow behavior in terrain-inclined pipelines for wet natural gas transportation	207

NUMERICS, METHODS & CODE DEVELOPMENT	213
Innovative computing for industrially-relevant multiphase flows	215
Development of GPU parallel multiphase flow solver for turbulent slurry flows in cyclone.....	223
Immersed boundary method for the compressible Navier–Stokes equations using high order summation-by-parts difference operators	233
Direct numerical simulation of coupled heat and mass transfer in fluid-solid systems	243
A simulation concept for generic simulation of multi-material flow, using staggered Cartesian grids.....	253
A cartesian cut-cell method, based on formal volume averaging of mass, momentum equations.....	265
SOFT: a framework for semantic interoperability of scientific software	273
 POPULATION BALANCE	 279
Combined multifluid-population balance method for polydisperse multiphase flows	281
A multifluid-PBE model for a slurry bubble column with bubble size dependent velocity, weight fractions and temperature.....	285
CFD simulation of the droplet size distribution of liquid-liquid emulsions in stirred tank reactors	295
Towards a CFD model for boiling flows: validation of QMOM predictions with TOPFLOW experiments	301
Numerical simulations of turbulent liquid-liquid dispersions with quadrature-based moment methods.....	309
Simulation of dispersion of immiscible fluids in a turbulent couette flow	317
Simulation of gas-liquid flows in separators - a Lagrangian approach.....	325
CFD modelling to predict mass transfer in pulsed sieve plate extraction columns	335
 BREAKUP & COALESCENCE	 343
Experimental and numerical study on single droplet breakage in turbulent flow	345
Improved collision modelling for liquid metal droplets in a copper slag cleaning process	355
Modelling of bubble dynamics in slag during its hot stage engineering.....	365
Controlled coalescence with local front reconstruction method	373
 BUBBLY FLOWS	 381
Modelling of fluid dynamics, mass transfer and chemical reaction in bubbly flows	383
Stochastic DSMC model for large scale dense bubbly flows.....	391
On the surfacing mechanism of bubble plumes from subsea gas release.....	399
Bubble generated turbulence in two fluid simulation of bubbly flow	405
 HEAT TRANSFER	 413
CFD-simulation of boiling in a heated pipe including flow pattern transitions using a multi-field concept	415
The pear-shaped fate of an ice melting front	423
Flow dynamics studies for flexible operation of continuous casters (flow flex cc).....	431
An Euler-Euler model for gas-liquid flows in a coil wound heat exchanger.....	441
 NON-NEWTONIAN FLOWS.....	 449
Viscoelastic flow simulations in disordered porous media	451
Tire rubber extrudate swell simulation and verification with experiments	459
Front-tracking simulations of bubbles rising in non-Newtonian fluids.....	469
A 2D sediment bed morphodynamics model for turbulent, non-Newtonian, particle-loaded flows.....	479

METALLURGICAL APPLICATIONS.....	491
Experimental modelling of metallurgical processes	493
State of the art: macroscopic modelling approaches for the description of multiphysics phenomena within the electroslag remelting process	499
LES-VOF simulation of turbulent interfacial flow in the continuous casting mold	507
CFD-DEM modelling of blast furnace tapping	515
Multiphase flow modelling of furnace tapholes	521
Numerical predictions of the shape and size of the raceway zone in a blast furnace.....	531
Modelling and measurements in the aluminium industry - Where are the obstacles?	541
Modelling of chemical reactions in metallurgical processes.....	549
Using CFD analysis to optimise top submerged lance furnace geometries	555
Numerical analysis of the temperature distribution in a martensic stainless steel strip during hardening.....	565
Validation of a rapid slag viscosity measurement by CFD.....	575
Solidification modeling with user defined function in ANSYS Fluent.....	583
Cleaning of polycyclic aromatic hydrocarbons (PAH) obtained from ferroalloys plant.....	587
Granular flow described by fictitious fluids: a suitable methodology for process simulations	593
A multiscale numerical approach of the dripping slag in the coke bed zone of a pilot scale Si-Mn furnace.....	599
 INDUSTRIAL APPLICATIONS	 605
Use of CFD as a design tool for a phosphoric acid plant cooling pond	607
Numerical evaluation of co-firing solid recovered fuel with petroleum coke in a cement rotary kiln: Influence of fuel moisture	613
Experimental and CFD investigation of fractal distributor on a novel plate and frame ion-exchanger	621
 COMBUSTION	 631
CFD modeling of a commercial-size circle-draft biomass gasifier.....	633
Numerical study of coal particle gasification up to Reynolds numbers of 1000.....	641
Modelling combustion of pulverized coal and alternative carbon materials in the blast furnace raceway	647
Combustion chamber scaling for energy recovery from furnace process gas: waste to value	657
 PACKED BED.....	 665
Comparison of particle-resolved direct numerical simulation and 1D modelling of catalytic reactions in a packed bed	667
Numerical investigation of particle types influence on packed bed adsorber behaviour	675
CFD based study of dense medium drum separation processes	683
A multi-domain 1D particle-reactor model for packed bed reactor applications.....	689
 SPECIES TRANSPORT & INTERFACES	 699
Modelling and numerical simulation of surface active species transport - reaction in welding processes	701
Multiscale approach to fully resolved boundary layers using adaptive grids.....	709
Implementation, demonstration and validation of a user-defined wall function for direct precipitation fouling in Ansys Fluent.....	717

FREE SURFACE FLOW & WAVES	727
Unresolved CFD-DEM in environmental engineering: submarine slope stability and other applications.....	729
Influence of the upstream cylinder and wave breaking point on the breaking wave forces on the downstream cylinder	735
Recent developments for the computation of the necessary submergence of pump intakes with free surfaces	743
Parallel multiphase flow software for solving the Navier-Stokes equations	752
 PARTICLE METHODS	 759
A numerical approach to model aggregate restructuring in shear flow using DEM in Lattice-Boltzmann simulations	761
Adaptive coarse-graining for large-scale DEM simulations.....	773
Novel efficient hybrid-DEM collision integration scheme.....	779
Implementing the kinetic theory of granular flows into the Lagrangian dense discrete phase model.....	785
Importance of the different fluid forces on particle dispersion in fluid phase resonance mixers	791
Large scale modelling of bubble formation and growth in a supersaturated liquid.....	798
 FUNDAMENTAL FLUID DYNAMICS	 807
Flow past a yawed cylinder of finite length using a fictitious domain method	809
A numerical evaluation of the effect of the electro-magnetic force on bubble flow in aluminium smelting process.....	819
A DNS study of droplet spreading and penetration on a porous medium.....	825
From linear to nonlinear: Transient growth in confined magnetohydrodynamic flows.....	831

INNOVATIVE COMPUTING FOR INDUSTRIALLY-RELEVANT MULTIPHASE FLOWS

**Damir JURIC^{1*}, Jalel CHERGUI¹, Seungwon SHIN²,
Lyes KAHOUADJI³, Richard V. CRASTER⁴, Omar K. MATAR³**

¹Laboratoire d'Informatique pour la Mécanique et les Sciences de l'Ingénieur (LIMSI),

Centre National de la Recherche Scientifique (CNRS), Rue John von Neumann, 91405 Orsay, FRANCE

²Department of Mechanical and System Design Engineering, Hongik University, Seoul, 121-791 SOUTH KOREA

³Department of Chemical Engineering, Imperial College London,
South Kensington Campus, London SW7 2AZ, UK

⁴Department of Mathematics, Imperial College London,
South Kensington Campus, London SW7 2AZ, UK

* E-mail: damir.juric@limsi.fr

ABSTRACT

The ability to predict the behaviour of multiphase flows accurately, reliably, and efficiently addresses a major challenge of global economic, scientific, and societal importance. These flows are central to virtually every processing and manufacturing technology. Significant advances have been made in the numerical methods to simulate these flows; examples of these include the use of Large Eddy Simulations to simulate turbulence, and interface-capturing or tracking techniques to deal with the free surface. These codes have made progress in simulating the interaction of a turbulent flow field with an interface, however, there remains a large gap between what is achievable computationally and 'real-life' systems. We will present the latest on the modelling framework that we are currently developing within the Multi-scale Examination of MultiPhase physics in flowS (MEMPHIS) programme that will enable the use of numerical simulations as a reliable design tool. The framework features Front-Tracking/Level-Set hybrids, an Immersed Boundary approach to Fluid-Structure Interaction and sophisticated multi-scale, multi-physics models. The code we call BLUE is fully parallelised and can run on various platforms: from laptops to supercomputers (on over 250,000 cores). This allows the user the flexibility to choose between a quick 'answer' with a degree of uncertainty common to engineering applications or a high-fidelity solution, for targeted cases, that requires more time. BLUE also has built-in, user-friendly meshing capabilities that allow rapid construction of complex geometries. We present a number of simulations of problems of interest to process industries and biomedical applications, which include the design of container-filling processes, two-fluid mixing with a rotating impeller, high-speed atomization, microfluidic droplet encapsulation, falling film reactors featuring non-Newtonian fluids, and surfactant-driven non-isothermal flows.

Keywords: CFD, Multiphase flow, Surfactants, Chemical reactors, Atomization, Filling, Mixing, Microfluidics, Non-Newtonian fluids, Fluid Structure Interaction.

NOMENCLATURE

Greek Symbols

- ρ Mass density, [kg/m³].
- μ Dynamic viscosity, [kg/m.s].
- κ Curvature, [m⁻¹].
- σ Surface tension, [kg/s²].
- δ Dirac delta function, [m⁻³].
- α Arrhenius exponent
- $\dot{\gamma}$ Shear rate, [s⁻¹].

Latin Symbols

- t Time, [s].
- P Pressure, [Pa].
- T Temperature, [K].
- \mathbf{u} Fluid velocity, [m/s].
- \mathbf{V} Interface velocity, [m/s].
- \mathbf{g} Gravitational acceleration, [m/s²].
- \mathbf{n} Normal vector.
- n Power-law index.
- I Indicator function.
- \mathbf{F} Force per unit volume, [N/m³].
- N_c Number of computation cores.
- T_c Elapsed computation time.

Sub/superscripts

- 1 Fluid phase 1.
- 2 Fluid phase 2.
- ref Reference value for parallel performance.
- α Reference value for Arrhenius temperature.
- 0 Zero value for non-Newtonian viscosity.
- ∞ Infinite value for non-Newtonian viscosity.

INTRODUCTION

It is very common in nature as in industrial processes that two or more phases are present simultaneously. One of the most striking examples is probably the aerodynamic breakup atomization caused by shear stresses at the liquid-gas interface. This process consists of a liquid jet projected at high speed in a gas that destabilizes gradually until breaking up into a myriad of droplets. This mechanism, which is widely used in fuel injection or perfumery, for example, is only one aspect of a broad class of phenomena that can be gathered under the name of multiphase flows. General fluid-fluid interfaces are found in an extraordinary variety of situations and scales such as free-surface waves, jets, bubbles and drops just to name a few examples.

From a numerical perspective, the typical issues faced in multiphase flows lead immediately to questions such as: What is the actual shape of the interface or what are the interactions between the phases? In the wide field of multiphase flow, analytical approaches are useful but extremely limited to the most trivial cases. The natural extension is direct numerical simulation, helped by the continuing growth of information technology resources. Such flows are generally three-dimensional and require advanced numerical methods for many reasons. First, physical parameter discontinuities at the interface require particular techniques and several popular methods could be chosen such as Volume of Fluid (VOF) (Hirt and Nichols, 1981), Level Set (Osher and Sethian, 1988), Front Tracking (Unverdi and Tryggvason, 1992) or their recently developed hybrid combinations. The history of the development and descriptions of such methods for multiphase flows is thoroughly covered in Tryggvason et al. (2011). The discretized systems involve different and widely ranging spatio-temporal scales and therefore a large number of degrees of freedom. It is often necessary to scan the parameter space to study robustness of a system. Our approach in the code BLUE is based on an innovative hybridization of the Front-Tracking and Level Set methods which is fully parallelized and able to run on a variety of computer architectures (Shin et al. 2017a). Below we briefly describe the techniques implemented in BLUE, discuss the code's parallel performance and present a variety of simulation results in various challenging multiphase flow regimes.

DESCRIPTION OF THE CODE BLUE

In this section, we will describe the basic solution procedure for the Navier-Stokes equations with a brief explanation of the hybrid interface method implemented in BLUE. Details of the numerical implementation can be found in several articles by Shin and Juric (2002, 2007, 2009a, 2009b), Shin (2007) and Shin et al. (2011, 2017a).

The governing equations for transport of an incompressible two-phase flow can be expressed by a single field formulation:

Continuity equation

$$\nabla \cdot \mathbf{u} = 0$$

(1)

Momentum equation

$$\rho \left(\frac{\partial \mathbf{u}}{\partial t} + \mathbf{u} \cdot \nabla \mathbf{u} \right) = -\nabla P + \nabla \cdot \mu (\nabla \mathbf{u} + \nabla \mathbf{u}^T) + \rho \mathbf{g} + \mathbf{F}$$

(2)

where \mathbf{u} is the velocity, P the pressure, \mathbf{g} the gravitational acceleration and \mathbf{F} the local surface tension force at the interface and is described by the formulation:

$$\mathbf{F} = \sigma \kappa_H \nabla I$$

(2)

where I is the indicator function which is zero in one phase and one in the other phase, resolved with a sharp but smooth transition across 3 to 4 grid cells and is essentially a numerical Heaviside function generated using a vector distance function computed directly from the tracked interface (Shin and Juric, 2009a). This formulation was shown to essentially eliminate the spurious currents which had plagued most numerical techniques for surface-tension driven flows. κ_H is twice the mean interface curvature field calculated on the Eulerian grid using:

$$\kappa_H = \frac{\mathbf{F}_L \cdot \mathbf{G}}{\sigma \mathbf{G} \cdot \mathbf{G}}$$

(4)

where

$$\mathbf{F}_L = \int_{\Gamma(t)} \sigma \kappa_f \mathbf{n}_f \delta_f(\mathbf{x} - \mathbf{x}_f) ds$$

(5)

and

$$\mathbf{G} = \int_{\Gamma(t)} \mathbf{n}_f \delta_f(\mathbf{x} - \mathbf{x}_f) ds$$

(6)

Here \mathbf{x}_f is a parameterization of the interface, $\Gamma(t)$, and $\delta(\mathbf{x} - \mathbf{x}_f)$ is a Dirac distribution that is non-zero only when $\mathbf{x} = \mathbf{x}_f$. \mathbf{n}_f is the unit normal vector to the interface and ds is the length of the interface element. κ_f is again twice the mean interface curvature but obtained from the Lagrangian interface structure. The geometric information, unit normal, \mathbf{n}_f and length of the interface element, ds , in \mathbf{G} are computed directly from the Lagrangian interface and then distributed onto an Eulerian grid using the discrete delta function. The details follow Peskin's (1977) pioneering immersed boundary approach.

The Lagrangian interface is advected by integrating

$$\frac{d\mathbf{x}_f}{dt} = \mathbf{V}$$

(7)

with a second order Runge-Kutta method where the interface velocity, \mathbf{V} , is interpolated from the Eulerian velocity. Material properties such as density or viscosity are defined in the entire domain with the aid of the indicator function, $I(\mathbf{x}, t)$:

$$\rho(\mathbf{x}, t) = \rho_1 + (\rho_2 - \rho_1)I(\mathbf{x}, t)$$

(8)

$$\mu(\mathbf{x}, t) = \mu_1 + (\mu_2 - \mu_1)I(\mathbf{x}, t) \quad (9)$$

where the subscripts 1 and 2 stand for the respective phases.

The code's solution structure consists of essentially two main modules:

- A module for solution of the incompressible Navier-Stokes equations as well as transport of energy, species or surfactant when applicable.
- A module for the interface solution including tracking the Lagrangian mesh of triangular interface elements, initialization and reconstruction of the interface when necessary.

The parallelization of the code is based on an algebraic domain decomposition technique. The code is written in the computing language Fortran 2008 and communications are managed by data exchange across adjacent subdomains via the Message Passing Interface (MPI) protocol. The Navier-Stokes solver computes the primary variables of velocity, \mathbf{u} , and pressure, P , on a fixed and uniform Eulerian mesh by means of the well-known projection method (Chorin, 1968, Temam, 1968, Goda, 1979). Depending on the physical problem, numerical stability requirements and user preferences, the user has a choice of explicit or implicit time integration to either first or second-order. For the Eulerian 3D spatial discretisation we use the staggered mesh, MAC method pioneered by Harlow and Welch (1965). All spatial derivative operators are evaluated using standard centered differences, except in the nonlinear term where we use a second-order Essentially-Non-Oscillatory (ENO) scheme (Shu and Osher, 1989 and Sussman et al., 1998).

We use a multigrid iterative method for solving the elliptic pressure Poisson equation

$$\nabla \cdot \left(\frac{1}{\rho} \nabla P \right) = S \quad (10)$$

where S denotes the source term and is a function of the non-projected velocities, interfacial tension and any body or external forces. In the case of two-phase flow with large density ratio the now non-separable Poisson equation is solved for the pressure by a modified multigrid procedure implemented for distributed processors. We have developed a modified parallel 3D V-cycle multigrid solver based on the work of Kwak and Lee (2004). The solver incorporates a parallel multigrid procedure whose restriction and prolongation operators are not associated with each other, contrary to what is commonly used. This method has been successfully implemented to solve 3D elliptic equations where coefficients can be highly discontinuous (see Wesseling, 1988). The procedure can handle large density discontinuities. The key features of the modified multigrid implementation can be summarized as: (i) cell centered second order finite difference approximation of Eq. (10), (ii) Harmonic approximation of the discontinuous coefficient $1/\rho$ (iii) linear interpolation of the residual during the restriction process, (iv) cell flux

conservation of the error on coarse grids during the prolongation process, (v) a parallel Red-Black SOR technique to relax the linear systems on fine grids and (vi) solution of the error using a parallel GMRES algorithm on the coarsest grid. Further detail is described in Shin et al. (2017a).

Code BLUE Performance

There are two ways to evaluate the performance of parallel codes. The first method is called ‘‘heavy scaling’’ parallel performance which is based on program execution timings with varying number of cores (processors) while keeping the global mesh resolution fixed. The second method is called ‘‘weak scaling’’ based on program execution timings with varying number of cores while keeping the local (subdomain) resolution fixed. In BLUE, we are more concerned with the latter for two main reasons: (i) on large supercomputers such as the IBM BlueGene each core has a small memory of 512MB, and (ii) we are more concerned with using the finest global mesh resolution while increasing the number of cores (subdomains) instead of increasing the local mesh resolution. BLUE has been successfully run on over 250k cores on the IBM BlueGene/Q machine at IDRIS in Orsay, France with excellent linear scalability performance as shown in Fig. 2 for the case of drop splash on a thin film in Fig. 1 (Shin et al., 2017a). Fixing $32 \times 32 \times 32$ as the resolution per core and using up to $8192 = 16 \times 16 \times 32$ cores gives a global resolution of $512 \times 512 \times 1024$. The speedup and efficiency of BLUE for weak scaling is defined as:

$$\text{Speedup} = \frac{N_c}{N_{c_{ref}}} \text{Efficiency} \quad (11)$$

where N_c is the number of cores, $N_{c_{ref}}$ is the reference number of cores (here 128) and Efficiency is defined as

$$\text{Efficiency} = \frac{T_{c_{ref}}}{T_c} \quad (12)$$

where $T_{c_{ref}}$ is the elapsed time measured from $N_{c_{ref}} = 128$ cores. T_c is the elapsed time measured for $N_c = 512, 1024, 2048, 4096, \text{ or } 8192$ cores, respectively. We show the speedup with number of cores in Fig. 2 (top). The scalability of the code is sufficient to overcome communication overhead as the number of cores increases. Up to 8192 cores, speedup is linear. With 8192 cores, the code runs 42 times faster than with 128 reference cores if the global mesh resolution would have been fixed to $512 \times 512 \times 1024$. The efficiency, shown in Fig. 2 (bottom), demonstrates that the average core utilization is about 68% and is maintained constant up to 8192 cores. For less physically demanding cases, the efficiency of BLUE reaches over 90%. In all cases, the performance timings we gather are for code run times over many thousands of time steps. We note that parallel performance is highly dependent on, among many other things, the physical case simulated as well as the machine, thus comparisons between different codes, cases or machines must be conducted and interpreted with a great deal of caution.

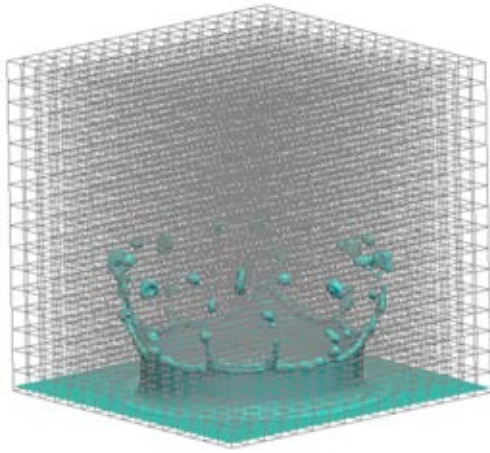


Figure 1: Water drop impact onto a thin film of water. 4096 core parallel computation.

we intend to perform complete rigorous investigations and mesh refinement studies in the future. Nevertheless, in the past several years we have gained considerable confidence in the fidelity of the code when comparing simulation results to experimental studies and analytical benchmarks. During the code development, validation and verification process, we maintain a growing test suite of more than two dozen single- and multiphase flow benchmark solutions with which simulations using BLUE are compared.

Fig. 1 shows a snapshot of the canonical droplet splash phenomenon. Here a 9mm diameter drop of water falling through air impacts a 1mm thick water film at 2.2 m/s creating an annular crown which ruptures and ejects small droplets at its rim. The simulation is performed on $16 \times 16 \times 16 = 4096$ subdomains (processor cores). Each subdomain is resolved by a $32 \times 32 \times 32$ grid. The global resolution is thus 512^3 .

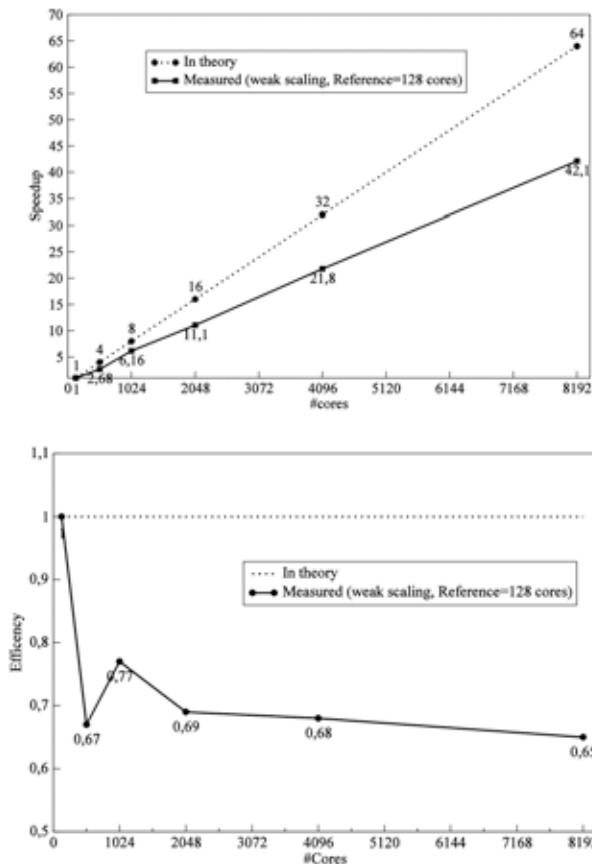


Figure 2: (Top): BLUE speedup on IBM BlueGene/Q for drop splash on a free surface. Performance increase with number of cores. (Bottom): BLUE efficiency on IBM BlueGene/Q for drop splash on a free surface. Efficiency vs. number of cores.

RESULTS

In order to demonstrate the range of applicability of BLUE to many different industrially-relevant multiphase flow scenarios, we present a variety of examples of both small-scale laptop (typically 8 core) calculations as well as massively parallel computations on thousands of cores. The very recent simulations presented here are presented as demonstrator, proof-of-concept simulations which explore flexible use of the code toward engineering design scenarios and for which

In Fig. 3 we demonstrate the simulation of flow in a complex solid geometry where a fluid 500 times more viscous than water exits a nozzle at 30 mL/s and fills a 6mm inner diameter mug and its hollow handle. The annular nozzle and mug were quickly constructed in BLUE by combining simple geometric forms without using a body-fitted mesh but rather using Immersed Boundary techniques. The simulation was conducted to demonstrate the capability of BLUE to deliver quick laptop simulations (~2 hour simulation time) of complex flows on a rather coarse $64 \times 64 \times 128$ mesh, while still capturing the essential features of the filling process.



Figure 3: Container filling with complex geometry. Simulation on 8 cores.

In the simulation shown in Fig. 4 we construct a complex microfluidic cross-junction to the exact dimensions of the experimental cell geometry, again using the Immersed Boundary technique. The main

channel branches have a width of 390 microns and a depth of 190 microns. In this three-phase flow, oil flows into the horizontal side branches which focus the aqueous stream entering from the top branch. Within this aqueous stream, a third oil phase is simultaneously introduced. This combined stream descends into the focusing junction whereupon the stream pinches further in the downstream branch to produce a drop of oil encapsulated within a drop of water.

In Fig. 5, a 12.5 cm deep layer of water is agitated by the action of an impeller spinning at 100 rotations per second. The resulting vortex causes the air/water surface to descend toward the impeller blades. Here we compute on a 64x64x128 mesh using 16 cores. Higher resolution would be necessary to capture the details of further entrainment of the free surface and formation of small bubbles.

The simulation in Fig. 6 is inspired by the experimental studies of jet atomization by Marmottant and Villermaux (2004) using an annular injector of 7.8 mm inner diameter and an annular gap of 1.7 mm. Our simulation results were generated on a 256x256x1024 mesh using 2048 cores. For this case, a liquid jet flows out of the centre of the nozzle at 0.5 m/s while the gas flows from the annulus at a much higher speed of 15 m/s inducing wave formation on the liquid jet surface with subsequent ligament formation and breakup into droplets. The results are qualitatively very similar to the experiment and a further quantitative comparison of the spray characteristics is being undertaken.

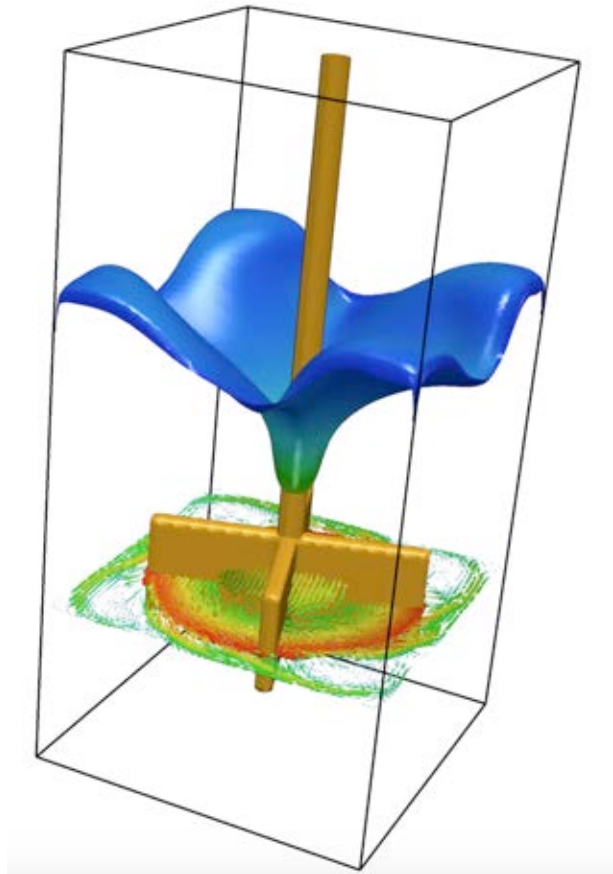


Figure 5: Rotating impeller with free surface deformation.

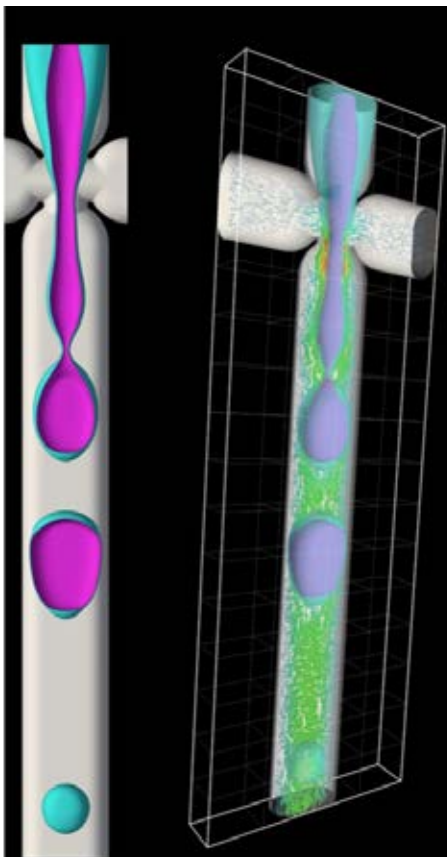


Figure 4: Microfluidic encapsulation. An example of a three-phase simulation.

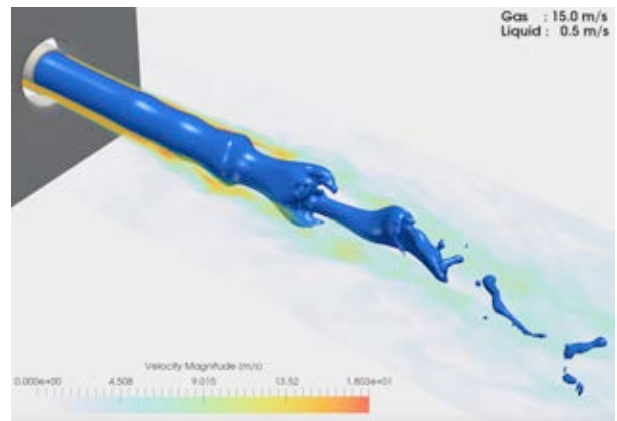


Figure 6: Jet atomization simulation on 2048 cores.

An annular falling film is studied in Fig. 7. Here an initially 4 mm thick liquid film falls downward inside of a 32.4 mm diameter solid tube together with a co-current flow of air in the core of the tube. The liquid is a non-Newtonian, shear-thinning fluid obeying a non-isothermal Carreau law with viscosity defined as:

$$\mu = H(T) \left(\mu_{\infty} + \frac{\mu_0 - \mu_{\infty}}{\left[1 + (\dot{\gamma}\lambda)^2\right]^{\frac{1-n}{2}}} \right) \quad (13)$$

where $\dot{\gamma}$ is the shear rate, n is the power-law index, λ is the time constant and μ_0 and μ_∞ are, respectively, the zero- and infinite-shear viscosities. $H(T)$ is the Arrhenius law temperature dependence:

$$H(T) = \exp \left[\alpha \left(\frac{1}{T - T_0} - \frac{1}{T_\alpha - T_0} \right) \right] \quad (14)$$

where T is the temperature of the liquid, α is the ratio of the activation energy to the thermodynamic constant. T_α is a reference temperature for which $H(T) = 1$. T_0 is the temperature shift and corresponds to the lowest temperature that is thermodynamically acceptable. In this simulation we use $n=0.1$ corresponding to a shear thinning fluid, $\lambda=0.1$ s, $\mu_0=0.009$ kg/m.s and $\mu_\infty= 10^{-7}$ kg/m.s. In the Arrhenius relation, we use $\alpha=0.5$, $T_0=0$ K and $T_\alpha=300$ K. The simulation was performed on 8 cores with a 64x64x256 grid. For this relatively thick initial liquid layer, we observe quite strong interface deformation leading to ligament formation and bubble entrainment. In further annular falling film simulations, not shown here, we have studied the effect of soluble surfactant transport on flooding in counter-current flows (Shin et al., 2017b).

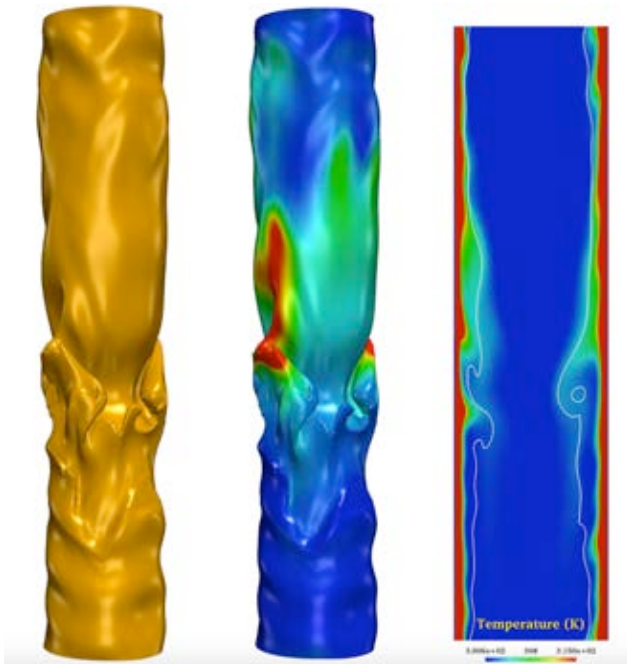


Figure 7: Annular falling film. Non-Newtonian fluid inside of a heated solid cylinder with co-current gas core flow. Simulation using the code BLUE on an 8 processor laptop.

CONCLUSION

We present BLUE a simulation and design tool for multiphase flows in industrial processes. We combine in BLUE recently developed innovative algorithms for high precision interface-tracking, novel multigrid and GMRES linear solvers and the immersed boundary

approach for meshless construction of solid objects and fluid-structure interaction. The code is fully parallelised and has been tested on a number of different architectures from laptops and small clusters to massively parallel HPC machines. BLUE has been written entirely from scratch to take advantage of modern object-oriented programming features, compiles and runs using MPI and is otherwise independent of any external software libraries. These advances have allowed simulations of industrially-relevant multiphase and multi-physics problems where complex interface dynamics, extreme density and viscosity differences, fluid rheology and chemistry pose great challenges. In this article, we have only presented a brief outline of the numerical techniques in BLUE, discussed the code's parallel performance and shown a small sample of simulation examples. The large range of spatial scales present in the drop splash or jet atomization cases necessitate very fine grids and benefit from large scale parallelism. However, many cases have been run on relatively coarse grids on a handful of cores in order to demonstrate that quick design type simulations on a laptop or desktop machine could be accessible while still retaining an excellent approximation of the main features in the flow process. Other capabilities of BLUE which we have not demonstrated here include surfactant-laden flows, flows with phase change in boiling or solidification, rotating flows subject to Coriolis and centrifugal forces, thermal and solutal Marangoni convection and input of CAD generated solid geometries. Continuing developments of BLUE will allow the ability to handle compressible flows and also incorporate adaptive mesh refinement.

ACKNOWLEDGEMENTS

This work is supported by (1) the Engineering & Physical Sciences Research Council, United Kingdom, through the MEMPHIS program grant (EP/K003976/1), (2) the Basic Science Research Program through the National Research Foundation of Korea (NRF) funded by the Ministry of Science, ICT and future planning (NRF-2014R1A2A1A11051346) and (3) by computing time at the Institut du Developpement et des Ressources en Informatique Scientifique (IDRIS) of the Centre National de la Recherche Scientifique (CNRS), coordinated by GENCI (Grand Equipement National de Calcul Intensif). Graphical visualizations are produced via ParaView.

REFERENCES

- CHORIN, J., (1968), "Numerical solution of the Navier-Stokes equations", *Mathematics of Computation*, **22**, 745-762.
- GODA, K., (1979), "A multistep technique with implicit difference schemes for calculating two- or three-dimensional cavity flows", *J. Comput. Phys.* **30**, 76-95.
- HARLOW, F.H. and WELCH, J.E., (1965), "Numerical calculation of time dependent viscous incompressible flow of fluid with free surface", *Physics of Fluids*, **8**, 2182-2189.
- HIRT, C. W. and NICHOLS, B. D., (1981), "Volume

of Fluid (VOF) method for the dynamics of free boundaries”, *J. Comput. Phys.*, **39**, 201-226.

KWAK, D. Y. and LEE, J. S., (2004), “Multigrid algorithm for the cell-centered finite-difference method ii: Discontinuous coefficient case”, *Numer. Meth. Part. Differ. Equ.* **20**, 723-741.

MARMOTTANT, P. and VILLERMAUX, E., (2004), “On spray formation”, *J. Fluid Mech.*, **498**, 73-111.

OSHER, S. and SETHIAN, J., (1988), “Fronts propagating with curvature-dependent speed: algorithms based on Hamilton-Jacobi formulations”, *J. Comput. Phys.*, **79**, 12-49.

PESKIN, C. S., (1977), “Numerical analysis of blood flow in the heart”, *J. Comput. Phys.* **25**, 220-252.

SHIN, S. and JURIC, D., (2002), “Modeling three-dimensional multiphase flow using a level contour reconstruction method for front tracking without connectivity”, *J. Comput. Phys.*, **180**, 427-470.

SHIN, S. and JURIC, D., (2007), “High order level contour reconstruction method”, *Journal of Mechanical Science and Technology*, **21**(2), 311-326.

SHIN, S., (2007), “Computation of the curvature field in numerical simulation of multiphase flow”, *J. Comput. Phys.* **222**, 872-878.

SHIN, S. and JURIC, D., (2009a), “A hybrid interface method for three-dimensional multiphase flows based on front-tracking and level set techniques”, *Int. J. Num. Meth. Fluids*, **60**, 753-778.

SHIN, S. and JURIC, D., (2009b), “Simulation of droplet impact on a solid surface using the level contour reconstruction method”, *Journal of Mechanical Science and Technology*, **23**, 2434-2443.

SHIN, S., YOON, I. and JURIC, D., (2011), “The Local Front Reconstruction Method for direct

simulation of two-and three-dimensional multiphase flows”, *J. Comput. Phys.*, **230**, 6605-6646.

SHIN, S., CHERGUI, J. and JURIC, D., (2017a), “A solver for massively parallel direct numerical simulation of three-dimensional multiphase flows”, *Journal of Mechanical Science and Technology*, to appear, arXiv 1410.8568.

SHIN, S., CHERGUI, J., JURIC, D., KAHOUADJI, L., MATAR, O. K. and CRASTER, R. V., (2017b), “An interface-tracking technique for multiphase flow with soluble surfactant”, *J. Comput. Phys.*, submitted. ArXiv 1702-02478.

SHU, C.-W. and OSHER, S., (1989), “Efficient implementation of essentially non-oscillatory shock capturing schemes II”, *J. Comput. Phys.*, **83**, 32-78.

SUSSMAN, M., FATEMI, E., SMEREKA and OSHER, S., (1998), “An improved level set method for incompressible two-phase flows”, *Computers and Fluids*, **27**, 663-680.

TEMAM, R., (1968), “Une méthode d'approximation de la solution des équations de Navier-Stokes”, *Bull. Soc. Math. France*, **96**, 115-152.

TRYGGVASON, G., SCARDOVELLI, R. and ZALESKI, S., (2011), “Direct Numerical Simulations of Gas-Liquid Multiphase Flows,” *Cambridge University Press*.

UNVERDI, S. O. and TRYGGVASON, G., (1992), “A front-tracking method for viscous, incompressible, multi-fluid flows”, *J. Comput. Phys.*, **100**, 25-37.

WESSELING, P., (1988), “Cell-centred multigrid for interface problems”, *J. Comput. Phys.*, **79**, 85-91.